Effect of Hexadecyltrimethyl-Ammonium Loaded Montmorillonite on The Cu Adsorption: Adsorption Surface Sites Involved

*César Fernández Morantes[1], Alejandra M Fernández Solarte[2], and Rosa M Torres Sánchez[1]**

[1]CETMIC-CCT La Plata - CIC, Camino Centenario y 506, (1897) M. B. Gonnet, La Plata, Argentina

[2]Fundación universitaria Los Libertadores. Cra. 16 # 63a-68, Bogotá Cundinamarca, Colombia

***Corresponding author:**

Rosa M Torres Sánchez

CETMIC-CCT La Plata - CIC, Camino Centenario y 506, (1897) M. B. Gonnet, La Plata, Argentina.,

Received : December 6, 2019
Published : December 20, 2019

ABSTRACT

NA raw montmorillonite (Mt) and two organo-montmorillonites (OMt) with different hexadecyltrimethyl-ammonium bromide (HDTMABr) was used to adsorb Cu^{2+}. The Cu^{2+} adsorption isotherms were performed, and Langmuir, Freundlich and SIPS mathematical models were evaluated. According to the R^2 term, the experimental data were appropriately described by SIPS models for all the samples. Thermal analysis of the OMt adsorbents and their Cu^{2+} adsorbed products indicated that HDTMA was associated with cation exchange and Van der Waals interactions to the Mt surface. The decrease of the de-surfactant temperature mainly for MH0.5-Cu respect to MH0.5 sample would indicate a weaker Van der Waals interactions of alkyl chains at the external surface by the Cu presence. The Cu^{2+} and the HDTMA entrance at the interlayer of Mt was evidenced by XRD analysis, where the cationic exchange process occurs. The zeta potential values behavior evidenced the importance of the external surface participation in the Cu^{2+} adsorption mainly for OMt samples.

Keywords: Copper, Clay, Organo-Montmorillonite, Surfactant, Adsorption.

INTRODUCTION

The pollution associated with different processes of the human, industrial and mining activities, can be localized in effluents with different content of toxic metals and/or organic pollutants. However, soil and water act as final sinks, the water contamination can affect populations of riverbanks areas and the quality of agricultural soils can also have consequences on the health status of the inhabitants [1,2].

Particularly, copper is an essential nutrient for human health, but excessive amounts can result in various pathologies and in severe cases death [3].

The concern for both, health and environment, has led to the development of a large number of researches aiming to remove these pollutants from water. The adsorption process is one of the technologically preferred treatments due to its effectiveness, versatility, low cost and simplicity. Among the wide variety of adsorbents materials, clays, and particularly montmorillonite (Mt), has been shown as strong candidate for the removal of heavy metal from wastewater [2,4-6] Their low cost place them among the preferred adsorbents for industrial treatments, in addition to its negative surface charge (originated by the isomorphic substitution balanced by exchangeable cations, mainly Na^+ and Ca^{2+}, located in the interlayer space) and high surface that lets an important removal of cationic contaminats. The adsorption of metal cations occurs via two different mechanisms that includes

DOI : https://doi.org/10.35702/msci.10004

cation exchange, in the interlayer with outer-sphere complexes formation and, secondly, on edge sites with variable charge on the external surfaces with formation of inner-sphere complexes through $Si–O^-$ and $Al–O^-$ groups at the clay particle edges [7]. The strong interaction involved generates a difficult and/or low-cost recovery of metals.

Particularly, although the Na-Mt sample reaches adsorption values for some heavy metals close to those of activated carbon (Uzun et al. 2000), additionally that Na-Mt is cheaper. When it is attempted to use it technologically in columns it fails due to its strong swelling capacity. The swelling capacity of Na-Mt can be eliminated by exchanging the Na^+ by Ca^{2+}, but the adsorption capacity value decreased to half of that found for Na-Mt [8].

The inorganic raw cations can also be exchanged by quaternary ammonium cations (QAC) to produce organo-montmorillonites (OMt) whose loading amount, alkyl substitutions, etc., change the initial structural and chemical parameters [9] and allowed them to adsorb heavy metals attaining different success [10-12] Although, the results involving the use of OMt to remove metals from effluents are noteworthy, there is still a need for a better understanding of the mechanisms involved in order to achieve their best recovery.

The aim of this study is to evaluate the Cu^{2+} adsorption capacity of OMt samples obtained from two different hexadecyltrimethyl-ammonium (HDTMA) exchange amount (50 and 100% of the cationic exchange capacity of the raw montmorillonite (Mt). In order to evaluate the surface sites and the strength of interactions involved, deep characterization of the Mt and OMt samples with and without Cu^{2+} has been performed by thermal analysis (DTA, TG/DTG), X-ray diffraction (XRD) and zeta potential measurements.

The knowledge acquired here will allow evaluating the strength of the interactions involved between the organo-clays and the metal cations that could help the greater recovery of the latter.

MATERIALS AND METHODS

Materials and chemicals

The montmorillonite (Mt) sample used in this study was from Rio Negro Province, provided by Castiglione Pes y Cia. Mineralogy analysis of Mt indicated that contained Na-montmorillonite (>99%), with quartz and feldspars as impurity, and chemical structural $[(Si_{3,89}Al_{0,11})(Al_{1,43}Fe^{3+}_{0,28}Mg_{0,30})O_{10}(OH)_2]^- Na^+_{0,41}$ by chemical analysis [13]. The cationic exchange capacity (CEC), determined by Cu-triethylenetetramine method, was 0.825 mmol/g clay, external specific surface area = 34 $m^2\ g^{-1}$ determined by N_2 adsorption and isoelectric point (IEP) = 2.7 [14].

The hexadecyltrimethylammonium (HDTMA; purity 98%) bromide and $CuNO_3.6H_2O$ (purity 99%) were purchased from Sigma Aldrich Co., and used as received.

The HDTMABr solubility in water is 50 mg mL^{-1}, MW = 364.5 g mol^{-1} and critical micelle concentrations (CMC) = 9 x 10^{-4} M [15].

Preparation of organo-montmorillonites

The synthesis of organo-montmorillonites (OMt) samples was performed according to the procedure previously described [14]. Briefly, the HDTMABr amount equivalent to 50 or 100 % CEC value of Mt was dissolved in 1 L of distilled water, and 10 g of Mt was slowly added and stirred (400 rpm) for 2 h at 60°C. The products attained were washed with distilled water to free them from bromide anions (tested by $AgNO_3$) and dried at 80°C. The OMt samples were labeled as MH0.5 and MH1, where 0.5 and 1 indicate the HDTMA concentration respect to the CEC of Mt.

Batch adsorption experiments

The retention of Cu^{2+} on Mt and OMt samples were investigated by batch adsorption experiments in initial concentrations (C_o) range of Cu^{2+} between 0 and 30 ppm, and mass concentration (2 g L^{-1}). The solutions *pH* was adjusted at *pH* = 5 by adding drops of HCl or KOH concentrated solutions. The dispersions were maintained at room temperature with continuous stirring for 24 h to attain equilibrium [16], and the adsorbents were separated by centrifugation at 15000 rpm for 15 min, dried for further characterization and labeled as Mt-Cu, MH0.5-Cu and MH1-Cu, respectively. The Cu^{2+} final concentration (C_f) was determined in the supernatant using Atomic Absorption Spectrometry (AAS) with an air/acetylene flame (Sens AA, from GBC Scientific Equipment).

The experimental isotherms were adjusted to Langmuir, Freundlich and Sips models.

The Langmuir model assumes a monolayer adsorption and can only occur at a finite number of definite localized sites. The nonlinear expression of the Langmuir isotherm model can be written as follows [17, 18]:

DOI : https://doi.org/10.35702/msci.10004

$$Q_e = \frac{Q_m K_L C_f}{1 + K_L C_f} \quad (1)$$

$$R_L = \frac{1}{1 + K_L C_0} \quad (2)$$

where *Qm* is the maximum adsorption capacity (mg g-1) and K_L is the Langmuir adsorption constant (L mg-1) that is related to adsorption energy and C_o is the lowest initial concentration of Cu^{2+}. The R_L parameter is the dimensionless separation factor that indicated the shape of the Langmuir isotherm.

Freundlich model can be used for non-ideal sorption that involves heterogeneous sorption. The nonlinear expression for the Freundlich isotherm model can be illustrated in equation 3 [17,18]:

$$Q_e = K_F . C_f^{(1/n)} \quad (3)$$

Where K_F is the Freundlich adsorption constant (L mg^{-1}) that is related to adsorption capacity, and *n* is the heterogeneity factor, while 1/*n* indicates the variation in adsorption as a function of concentration [19].

Sips models is a combination of Langmuir and Freundlich expressions for predicting the heterogeneous adsorption systems without limitation associated with the Freundlich isotherm model [17]. This model predicts that at low adsorbate concentration it behaves as the Freundlich model while at high concentrations a monolayer adsorption capacity occurs as indicates the Langmuir model. The nonlinear expression the Sips isotherm is illustrated in equation 4 [17,20]:

$$Q = \frac{Q_m (K_a C_f)^n}{1 + (K_a C_f)^n} \quad (4)$$

where, Q_m is the maximum adsorption capacity (mg g^{-1}), K_a is the affinity constant for adsorption (L mg^{-1}) and *n* is the Freundlich parameter that considers the system heterogeneity. The Sips isotherm is reduced to the Langmuir form for *n* = 1 when a homogeneous surface is considered.

METHODS

Thermogravimetric analysis (TGA) were conducted using a Rigaku TG 8121 Thermo plus EVO2 equip with alumina as a reference. Samples of 50 mg were placed in Al_2O_3 crucibles and heated from 30 to 800°C at a scanning rate of 10°C min^{-1} in air atmosphere.

The XRD patterns were obtained with a Bruker AXS D2 Phaser diffractometer, operated at 40 kV and 30 mA using CuK_α radiation and scanning parameters were counting time 10 s/step and 0.02° (2θ) step size, within range 2-12° (2θ). Samples were scanned on oriented form. Glass slides were covered with sample slurry to improve the precision of the peak values. These were prepared by drying for 48 h at room temperature and constant relative humidity (rh) of 0.56 [21].

Electrophoretic potentials were determined using Brookhaven 90Plus/Bi-MAS Multi Angle Particle Sizing, operated at: λ = 635 nm, 15 mW solid state laser, scatter angle = 90°, and temperature = 25°C and employing 10^{-3} M KCl as inert electrolyte and Pd electrodes. The electrophoretic mobility was converted automatically into a zeta potential values using the Smoluchowski equation [22]. To generate zeta potential versus pH curves, 40 mg of sample was dispersed in 40 mL KCl 10^{-3} M, used as inert electrolyte. The slurry was continuously stirred, and the suspension pH was adjusted using drops of HCl or KOH of different concentrations until equilibrium was attained (10 min).

RESULTS AND DISCUSSION

The Cu^{2+} sorption isotherms onto Mt, MH0.5 and MH1 samples are shown in **Figure 1** and the relevant parameters calculated from these models are listed in **Table 1**.

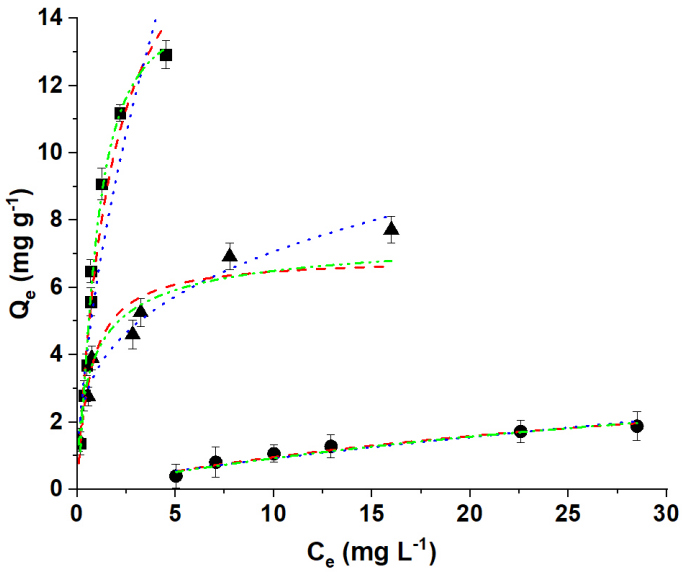

Figure 1: Cu^{2+} adsorption isotherm onto: (■) Mt; (▲) MH0.5 and (●) MH1 samples at pH 5. Lines represent the experimental data fitted to: (dash) Langmuir, (dot) Freundlich and (dash-dot) Sips models.

To better understand the adsorption of Cu^{2+} on Mt and OMt samples, Langmuir (equation 1), Freundlich (equation 2), and Sips (equation 3) isotherm models were used to quantitatively describe the adsorption isotherm of Cu^{2+}. A Cu^{2+} Q_{max} decrease was found with the HDMTA loading increase in agreement with previous data found by Ma et al. [23]. As indicated by the

DOI : https://doi.org/10.35702/msci.10004

R^2 values (**Table 1**), the adsorption isotherms of Cu^{2+} on Mt and OMts samples are better fitted with the Sips model than Langmuir or Freundlich ones [17,20]. Adsorption capacities toward Cu^{2+} in descending order of Q_{max} were Mt > MH0.5 > MH1 samples. The more efficient removal of Cu^{2+} attained by the Mt sample was due to the cation exchange reaction between the raw Na^+ and Cu^{2+} [8,23,24]. The decrease of Cu^{2+} adsorption on OMt samples, was attributed probably by Ma et al. (2016) to the lower exchange of copper cations with surfactant at the interlayer and they might be preferably adsorbed on the edge site of montmorillonite layers, as happened with Pb(II) adsorbed on similar OMt samples [25].

Table 1: Isotherm parameters obtained from Langmuir, Freundlich and Sips models fit experimental adsorption data.

Sample	Adsorption model	Parameters			
		Q_m (mg g^{-1})	K (L mg^{-1})	n	R^2
Mt-Cu	Langmuir	18.0 ±2.0	0.7 ±0.1	-----	0.972
	Freundlich	-----	6.8 ±0.5	1.9 ±0.2	0.9
	Sips	14.0 ±1.0	1.2 ±0.2	1.5 ±0.2	**0.989**
MH0.5-Cu	Langmuir	7.4 ±0.8	1.1 ±0.6	-----	0.858
	Freundlich	-----	3.6 ±0.2	3.5 ±0.3	0.951
	Sips	7.7 ±0.4	1.2 ±0.2	0.7 ±0.1	**0.967**
MH1-Cu	Langmuir	3.3 ±1.5	0.05 ±0.01	-----	0.945
	Freundlich	-----	0.22 ±0.05	1.5 ±0.2	0.926
	Sips	2.10 ±0.01	0.10 ± 0.01	1.91 ±0.01	**0.989**

In order to understand surface sites and interactions involved in the Cu^{2+} adsorption, Mt, OMt samples and their respective Cu^{2+} adsorbed (with 13,5 and 1 mg g^{-1} for Mt, MH0.5 and MH1 samples, respectively) products were characterized by thermal analysis (**Figure 2A**, **B** & **C**, respectively).

For Mt sample the DTG curve (**Figure 2A**), indicates a first broad peak located at 123°C assigned to a dehydration process of the water physiosorbed present in the external surface and interlayer space (with correspond to 13.3% mass loss), and a second one at 669°C attributed to the dehydration of hydroxyl groups [26]. The Cu^{2+} adsorption generated a shift of the first peak from 124 to 73°C, due to dehydration of the Cu(II) with its hydration sphere into the interlayer [27].

The HDTMA loading in OMt samples (**Figure 2B**) cause a temperature decrease of the first peak to 91°C (with 4.3% and 4.1% mass loss for MH0.5 and MH1 samples, in agreement with data found by Gamba et al. [14]. The surfactant presence originated two different decomposition temperatures, indicating the existence of different association mechanisms between the clay and the surfactant [28,29]. The first peak at around 285°C was associated with previous work to Van der Waals (VdW) interactions that occurred at the external surface [29]. Whilst the second peak at 399°C with a stronger interaction was attributed to cationic exchange process that takes place mainly at the interlayer [29]. The peak for dehydration of hydroxyl groups, found at 669°C in Mt sample, decreased to around 602°C for OMt assigned to oxidation of charcoal and formation of CO_2, whose temperature depends on experimental conditions and among others to the bonding between the clay and the organic compound [30].

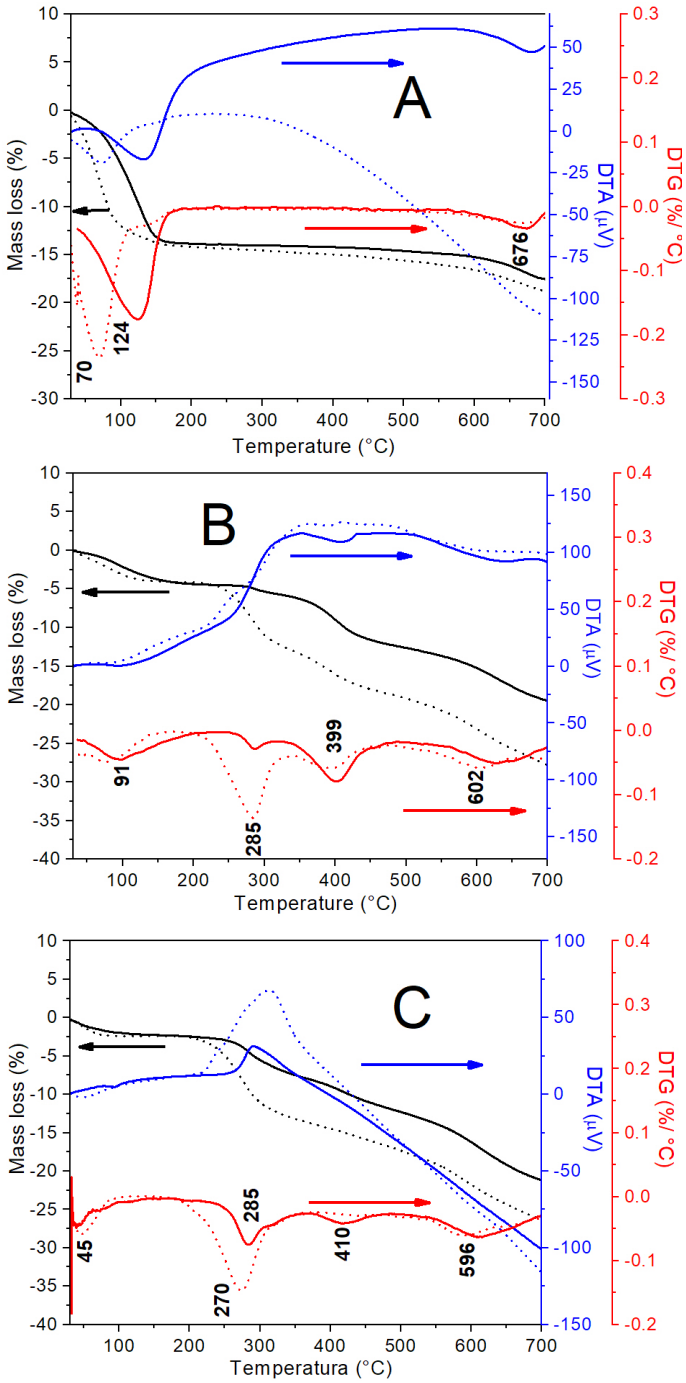

Figure 2: Curves DTA/TG-DTG for: A) Mt and Mt-Cu; B) MH1 and MH0.5 samples and. C) MH1-Cu and MH0.5-Cu. Amount of Cu^{2+} adsorbed were: 13 mg g^{-1}, 5 mg g^{-1} and 1 mg g^{-1} for Mt, MH0.5 and MH1 samples, respectively.

DOI : https://doi.org/10.35702/msci.10004

The Cu^{2+} adsorption on OMt samples (**Figure 2C**) produced a similar behavior of dehydration process to that found for Mt respect to Mt-Cu sample (**Figure 2A**). For both OMt samples, the temperature for the dehydration process decreased to 45°C. Particularly, the surfactant decomposition temperatures on OMt samples showed different behavior compare to the OMt samples that adsorbed Cu^{2+}. The peak assigned to cationic exchange process increased from 399°C to 410°C, irrespectively of the amount of Cu^{2+} adsorbed. The peak allocated to VdW interactions decreased from 285°C to 270°C for MH0.5, while remained at 285°C for MH1 sample. It is important to point out that, for both OMt-Cu samples, the peak intensities for both interactions increase with the surfactant amount loaded, as it happened to both OMt samples. In line with the behavior found for Mt samples the dehydration of hydroxyl group's peak decrease from 602°C to 595°C with the Cu^{2+} adsorption on OMt samples.

Summing up, DTG results indicated that the surfactant was loaded simultaneously by cation exchange and VdW at the Mt surfaces. The first interaction occurred on the internal surface of Mt (interlayer), while the second one appeared at edge sites with variable charge on the external surface of Mt, as it was previously identified for metal cations [7]. The modification of the de-surfactant process with further Cu^{2+} adsorption on OMt samples, could be indicative of VdW interaction strength alteration.

To attain more insights of the internal surface of Mt, changes of the basal reflection indicates the incorporation of the surfactant and/or the hydrated inorganic cations in the Mt interlayer, where the cationic exchange process occurs. Besides, as the neutrality of the interlayer remains with the cation exchange process [31], changes of the electrical surface charge was driven by modifications of the external surface [32]. Consequently, the surfactant VdW interactions at the external surface of Mt and the further Cu^{2+} adsorption could be evidenced by zeta potential values modification measured by the micro-electrophoresis method.

The basal reflection values obtained by XRD for samples with and without different Cu^{2+} adsorption are shown in **Figure 3**. For Mt sample (**Figure 3A**) the d001 value of 1.24 nm shifted to 0.25 and 0.19 nm with Cu^{2+} adsorption of 1.5 and 13 mg g^{-1} clay, respectively. As it was indicated in our previous work, these shifts were indicative of the preferred Cu^{2+} adsorption at the permanent charge sites of Mt sample [33]. The asymmetric peak shape observed (**Figure 3A**) when Cu^{2+} was adsorbed on Mt sample indicated a heterogeneous distribution in the interlayer generated by the presence of the different hydration spheres of Na^{+} or Cu^{2+} [34-36]. Particularly, when Cu^{2+} is at the Mt interlayer space, hexa-aqueous complexes $[Cu(H_2O)_6]^{2+}$ are formed [37, 38].

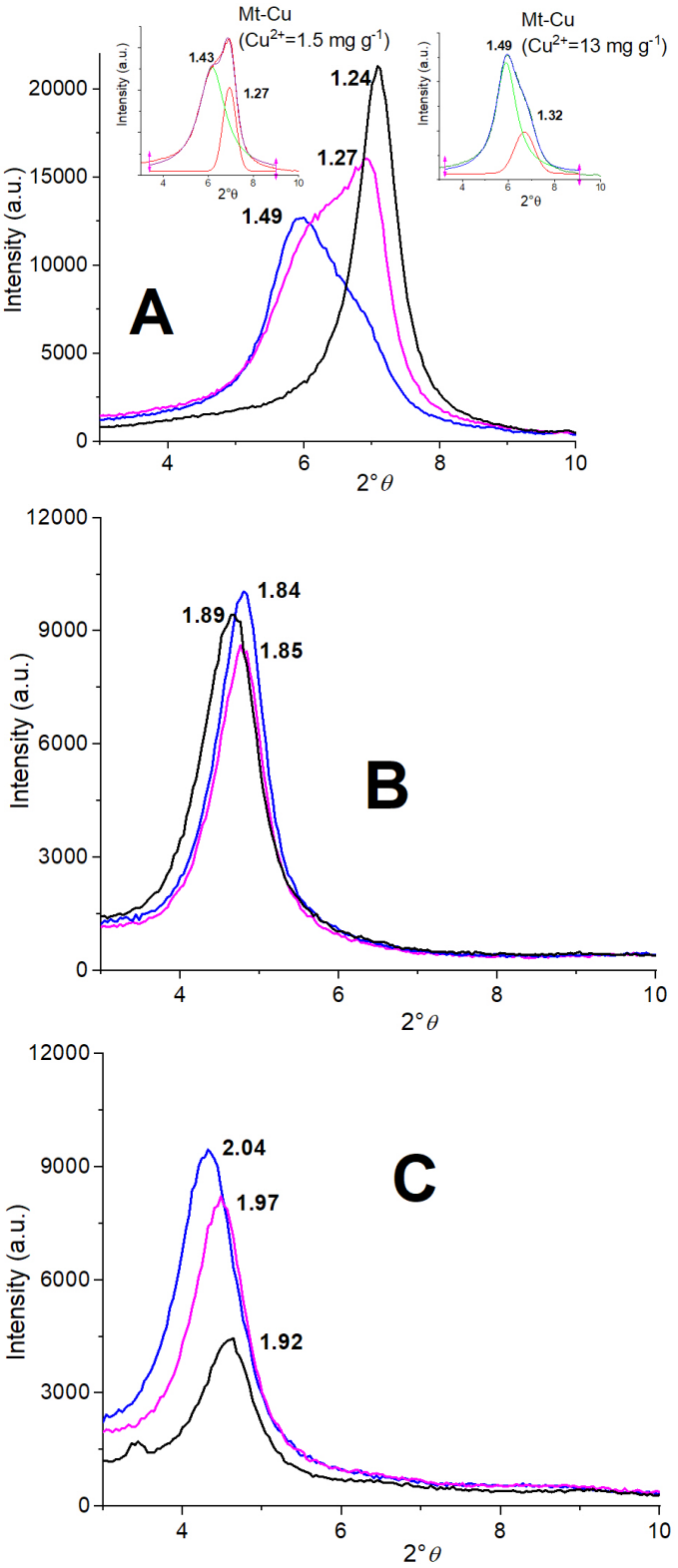

Figure 3: Partial XRD patterns for indicated samples: A) Mt (black line), Mt-Cu with 1.5 mg g^{-1} (pink line) and with 13 mg g^{-1} (blue line) Cu^{2+} adsorbed. Insets depicted the deconvolution peaks for indicated samples; B) MH0.5 (black line), MH0.5-Cu with 0.1 mg g^{-1} (pink line) and MH0.5-Cu with 5 mg g^{-1} (blue line) Cu^{2+} adsorbed, and C) MH1 (black line), MH1-Cu with 0.1 mg g^{-1} (pink line) and MH1-Cu with 1 mg g^{-1} (blue line) Cu^{2+} adsorbed.

The constant value obtained for the ratio of areas (3.81 and

DOI : https://doi.org/10.35702/msci.10004

4.17, for 1.5 and 13 mg of Cu^{2+} adsorbed by g clay, respectively) of the respective deconvoluted d001 peaks for Mt-Cu samples (**Figure 3A**), validated the important entry of Cu^{2+} in the interlayer, even at low Cu^{2+} concentration.

For MH0.5 and MH1 samples the surfactant interlayer entrance shifted the Mt initial d001 value from 1.24 nm to 1.89 nm and to 1.96 nm, respectively (**Figure 3B** & **C**), which indicated a bilayer surfactant arrangement [29,39]. However, for the MH0.5 sample, despite the different amount of Cu^{2+} adsorbed at each MH0.5-Cu samples (0.1 and 5 mg g^{-1} Cu^{2+}, respectively), the d001 value remained within the method error (**Figure 3B**) close to that of MH0.5 sample. This behavior could be assigned to a shielding effect produced by the presence of surfactant in the interlayer space of Mt. Notwithstanding, for MH1 sample despite the amount of Cu^{2+} adsorbed are lower than those of MH0.5-Cu samples (0.1 and 1 mg g^{-1} Cu^{2+}, respectively) the Cu^{2+} presence seems to modify slightly the surfactant arrangement at the interlayer.

To evaluate changes of electrical surface charge between the samples, also with the different amount of Cu^{2+} adsorbed, zeta potential vs pH curves were carried out (**Figure 4**) for Mt, MH0.5 and MH1 and same Cu^{2+} adsorbed products analyzed previously by XRD.

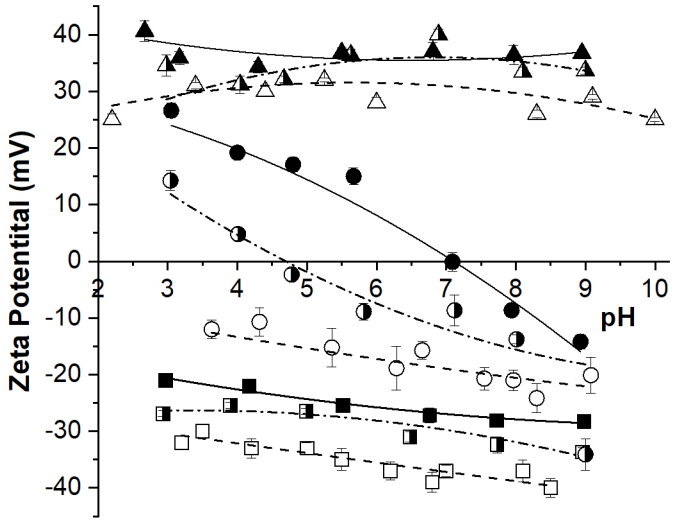

Figure 4: Zeta potential vs pH curves of (□) Mt, (○) MH0.5 and (△) MH1 samples without and with Cu^{2+} adsorbed. Symbols indicated: (empty) without, (half full) with minimum and (full) with maximum Cu^{2+} adsorbed. Minimum correspond to 1.5 mg g^{-1}, 0.1 mg g^{-1} and 0.1 mg g^{-1} and maximum to 13 mg g^{-1}, 5 mg g^{-1} and 1 mg g^{-1}, Cu^{2+} adsorbed for Mt, MH0.5 and MH1 samples, respectively.

The negative zeta potential (around −35 mV) observed at all pH studied for Mt sample is attributed to the predominance of the negative charges on the particle faces with respect to the positive charge coming from the edges [40,41]. While, the surfactant presence in the Mt sample cause a decrease in the negative zeta potential for the MH05 in all pH range, and reverse it to positive for MH1 sample [32].

The increase of Cu^{2+} adsorbed produced a direct decrease of the initial negative zeta potential value of Mt sample. The negative zeta potential value of Mt changed from -30 mV to around -25 mV and -20 mV, when 1.5 mg g^{-1} and 13 mg g^{-1} of Cu^{2+} was adsorbed.

For MH0.5 samples lower amounts of Cu^{2+} adsorbed than those found for Mt-Cu samples, produced higher variations of zeta potential values. The negative zeta potential value of MH0.5 sample changed from -15 mV to around 0 mV and reverse to +20 mV when 0.1 mg g^{-1} and 5 mg g^{-1} of Cu^{2+} was adsorbed. For MH1 sample despite the lower amounts of Cu^{2+} adsorbed (1 mg g^{-1} and 0.1 mg g^{-1}) than those found for the Mt-Cu and MH0.5-Cu samples, a maximum increase of about 5 mV with respect to the zeta potential value of the MH1 sample was found.

The behavior of the zeta potential values found evidenced the importance of the external surface participation in the Cu^{2+} adsorption.

CONCLUSIONS

In the present study raw montmorillonite (Mt) was converted into organo-montmorillonites by intercalating different loading amounts of hexadecyltrimethyl ammonium bromide, to test their capacity to adsorb Cu^{2+} from aqueous solution. The Sips mathematical model was the one that best suited the experimental data obtained for the adsorption of Cu^{2+} for all samples. Thermal analysis of the OMt adsorbents evidenced the simultaneous interaction of HDTMA to the internal and external Mt surface by cation exchange and with the edge sites with variable charge, respectively. The decrease of the de-surfactant temperature mainly for MH0.5-Cu sample respect to MH0.5 sample could be assigned to a weaker Van der Waals interaction of alkyl chains at the external surface by the Cu^{2+} presence. The variations of the interlayer thickness by XRD analysis validate the HDTMA and further Cu^{2+} entrance at the internal (or interlayer) surface of the Mt sample.

For Mt sample despite the high amount of Cu^{2+} adsorbed, up to 13 mg g^{-1} or 0.41 meq g^{-1}, the main interaction occurred at the interlayer surface site, as indicated XRD analysis. Because the CEC value of Mt sample is 0.825 meq g^{-1}, the maximum amount of Cu^{2+} adsorbed would only reach 50% of the CEC. However, the negative zeta potential decrease with the Cu^{2+} adsorption indicated that some inner-sphere complexes through $Si–O^-$ and $Al–O^-$ groups at the clay particle edges were

DOI : https://doi.org/10.35702/msci.10004

produced. While for the OMt samples, as it was found in our previous work for the fungicide thiabendazole, it is only the organic-free spaces of Mt surface that can interact with the Cu^{2+} and therefore increases the positive zeta potential despite the amount of Cu^{2+} adsorbed was less than in Mt sample.

Acknowledgments

Financial support of MINCyT- ANPCyT, PICT-2014-0585 is gratefully acknowledged. R.M.T.S. is member of CONICET and C.F.M. acknowledges CONICET fellowship.

The authors want to thank Dr. Ivan Romero Fonseca for his valuable help in editing this paper.

REFERENCES

1. Romic M, Romic D (2003) Heavy metals distribution in agricultural topsoils in urban area. Env Geol 43(7): 795-805.
2. Anyakora C, Ehianeta T, Umukoro O (2013) Heavy metal levels in soil samples from highly industrialized Lagos environment. Afr J Environ Sci Technol 7(9): 917-924.
3. Uriu-Adams JY, Keen CL (2005) Copper, oxidative stress, and human health. Mol Aspects Med 26(4-5): 268-298.
4. Bhattacharyya KG, Gupta SS (2008) Adsorption of a few heavy metals on natural and modified kaolinite and montmorillonite: a review. Adv Colloid Interface Sci 140(2): 114-131.
5. Abollino O, Giacomino A, Malandrino M and Mentasti E (2008) Interaction of metal ions with montmorillonite and vermiculite. Appl Clay Sci 38(3-4): 227-236.
6. Lakherwal D (2014) Adsorption of heavy metals: a review. IJESD 4(1): 41-48.
7. Zhu J, Cozzolino V, Pigna M, Huang Q, Caporale AG, et al. (2011) Sorption of Cu, Pb and Cr on Na-montmorillonite: competition and effect of major elements. Chemosphere 84(4): 484-489.
8. Alvarez-Ayuso E, Garcia-Sanchez A (2003) Removal of heavy metals from waste waters by natural and Na-exchanged bentonites. Clays Clay Miner 51(5): 475-480.
9. Zhu J, He H, Guo J, Yang D, Xie X (2003) Arrangement models of alkylammonium cations in the interlayer of HDTMA+ pillared montmorillonites. Chin Sci Bull 48(4): 368-372.
10. Yan D (2013) Researches on Adsorption Behaviour of Pb~(2+) with Organomontmorillonite. J Longyan Univ 5: 6.
11. Zhu L, Zhang L, Tang Y, Yang J (2013) Synthesis and Adsorption of Organo-Montmorillonite/Poly(Acrylic Acid) Superabsorbent Composite. Polym Polym Compos 21(1): 21-26.
12. Medhi H, Bhattacharyya KG (2017) Kinetic and mechanistic studies on adsorption of Cu(II) in aqueous medium onto montmorillonite K10 and its modified derivative. New J Chem 41(22): 13533-13552.
13. Magnoli AP, Tallone L, Rosa CAR, Dalcero AM, Chiacchiera SM, et al. (2008) Commercial bentonites as detoxifier of broiler feed contaminated with aflatoxin. Appl Surf Sci 40(1-4): 63-71.
14. Gamba M, Flores FM, Madejová J, Torres Sánchez RM (2015) Comparison of imazalil removal onto montmorillonite and nanomontmorillonite and adsorption surface sites involved: An approach for agricultural wastewater treatment. Ind Eng Chem Res 54(5): 1529-1538.
15. Rosen MJ, Kunjappu JT (2012) Surfactants and interfacial phenomena. [4th Ed.], John Wiley & Sons, New Jersey, USA, 616.
16. Eren E, Afsin B (2008) An investigation of Cu(II) adsorption by raw and acid-activated bentonite: A combined potentiometric, thermodynamic, XRD, IR, DTA study. J Hazard Mater 151(2-3): 682-691.
17. Foo KY, Hameed BH (2010) Insights into the modeling of adsorption isotherm systems. Chem Eng J 156(1): 2-10.
18. Armagan B, Toprak F (2013) Optimum isotherm parameters for reactive azo dye onto pistachio nut shells: Comparison of linear and non-linear methods. Pol J Environ Stud 22(4): 1007-1011.
19. Sanchez-Martin M, Rodriguez-Cruz M, Andrades M, Sanchez-Camazano M (2006) Efficiency of different clay minerals modified with a cationic surfactant in the adsorption of pesticides: influence of clay type and pesticide hydrophobicity. Appl Clay Sci 31(3): 216-228.
20. Jeppu GP, Clement TP (2012) A modified Langmuir-Freundlich isotherm model for simulating pH-dependent adsorption effects. J Contam Hydrol 129–130: 46-53.
21. Pacuła A, Bielańska E, Gaweł A, Bahranowski K, Serwicka EM (2006) Textural effects in powdered montmorillonite induced by freeze-drying and ultrasound pretreatment. Appl Clay Sci 32(1-2): 64-72.

DOI : https://doi.org/10.35702/msci.10004

22. Pecini EM, Avena MJ (2013) Measuring the isoelectric point of the edges of clay mineral particles: The case of montmorillonite. Langmuir 29(48): 14926-14934.

23. Ma L, Chen Q, Zhu J, Xi Y, He H, et al. (2016) Adsorption of phenol and Cu(II) onto cationic and zwitterionic surfactant modified montmorillonite in single and binary systems. Chem Eng J 283: 880-888.

24. Yuan GD, Theng BKG, Churchman GJ, Gates WP (2013) Clays and Clay Minerals for Pollution Control. [2nd Ed.] Elsevier, The Netherlands, 587-644.

25. Lee JJ, Choi J, Park JW (2002) Simultaneous sorption of lead and chlorobenzene by organobentonite. Chemosphere 49(10): 1309-1315.

26. Vazquez A, Lopez M, Kortaberria G, Martín L, Mondragon I (2008) Modification of montmorillonite with cationic surfactants. Thermal and chemical analysis including CEC determination 41(1): 24-36.

27. Hyun SP, Cho YH, Kim SJ, Hahn PS (2000) Cu (II) sorption mechanism on montmorillonite: an electron paramagnetic resonance study. J Colloid Interface Sci 222(2): 254-261.

28. Naranjo PM, Sham EL, Castellon ER, Torres Sanchez RM, Farfan Torres EM (2013) Identification and quantification of the interaction mechanisms between the cationic surfactant HDTMA-Br and montmorillonite. Clays Clay Miner 61(2): 98-106.

29. Fernandez Solarte AM, Villarroel-Rocha J, Fernandez Morantes C, Montes ML, Sapag K, et al. (2019) Insight into surface and structural changes of montmorillonite and organomontmorillonites loaded with Ag. C R Chim 22(2-3): 142-153.

30. Yariv S (2003) Differential thermal analysis (DTA) in the study of thermal reactions of organo–clay complexes. In: Ikan, R. (Eds) Natural and Laboratory-Simulated Thermal Geochemical Processes, Kluwer Academic, Dordrecht, 253-296.

31. Thomas F, Michot LJ, Vantelon D, Montarges E, Prelot B, Cruchaudet M, Delon DF (1999) Layer charge and electrophoretic mobility of smectites. Colloids Surf, A Physicochem Eng Asp 159(2-3): 351-358.

32. Bianchi AE, Fernandez M, Pantanetti M, Vina R, Torriani I, Torres Sanchez RM, et al. (2013) ODTMA+ and HDTMA+ organo-montmorillonites characterization: New insight by WAXS, SAXS and surface charge. App Clay Sci 83-84: 280-285.

33. Gamba M, Olivelli M, Lazaro-Martinez JM, Gaddi G, Curutchet G, Torres Sanchez RM (2017) Thiabendazole adsorption on montmorillonite, octadecyltrimethylammonium- and Acremonium sp.-loaded products and their copper complexes. Chem Eng J 320: 11-21.

34. Chalghaf R, Oueslati W, Ammar M, Rhaiem HB, Amara ABH (2012) Effect of an "in situ" hydrous strain on the ionic exchange process of dioctahedral smectite: Case of solution containing (Cu 2+, Co 2+) cations. App Surf Sci 258(22): 9032-9040.

35. Oueslati W, Rhaiem HB, Amara ABH (2011) XRD investigations of hydrated homoionic montmorillonite saturated by several heavy metal cations. Desalination 271(1-3): 139-149.

36. Oueslati W, Rhaiem HB, Amara ABH (2012) Effect of relative humidity constraint on the metal exchanged montmorillonite performance: An XRD profile modeling approach. App Surf Sci 261: 396-404.

37. Brtanova A, Madejova J, Bizovska V, Komadel P (2014) Utilization of near infrared spectroscopy for studying solvation properties of Cu-montmorillonites. Spectrochim Acta A Mol Biomol Spectrosc 123: 385-391.

38. Joseph-Ezra H, Nasser A, Mingelgrin U (2014) Surface interactions of pyrene and phenanthrene on Cu-montmorillonite. App Clay Sci 95: 348-356.

39. Schampera B, Tunega D, Solc R, Woche SK, Mikutta R, Wirth R, et al. (2016) External surface structure of organoclays analyzed by transmission electron microscopy and X-ray photoelectron spectroscopy in combination with molecular dynamics simulations. J Colloid Interf Sci 478: 188-200.

40. Missana T, Adell A (2000) On the applicability of DLVO theory to the prediction of clay colloids stability. J Colloid Interface Sci 230(1): 150-156.

41. Fernández M, Alba MD, Torres Sánchez RM (2013) Effects of thermal and mechanical treatments on montmorillonite homoionized with mono- and polyvalent cations: Insight into the surface and structural changes. Colloids Surf, A Physicochem Eng Asp 423: 1-10.

Copyright: Torres Sánchez RM, et al. ©2019. This is an open-access article distributed under the terms of the Creative Commons Attribution License, which permits unrestricted use, distribution, and reproduction in any medium, provided the original author and source are credited.

DOI : https://doi.org/10.35702/msci.10004